OPEN ACCESS

UNIVERSITY OF DUNDEE

University of Dundee

The Influence of Sea Level Rise on the Regional Interdependence of Coastal Infrastructure

Wang, Ruoqian; Stacey, Mark T.; Herdman, Live; Barnard, Patrick; Erikson, Li

RESEARCH ARTICLE

The Influence of Sea Level Rise on the Regional Interdependence of Coastal Infrastructure

Ruo-Qian Wang[1] (ID), **Mark T. Stacey**[2] (ID), **Liv Muir Meltzner Herdman**[3] (ID), **Patrick L. Barnard**[3] (ID), **and Li Erikson**[3] (ID)

[1]School of Science and Engineering, University of Dundee, Dundee, UK, [2]Department of Civil and Environmental Engineering, University of California, Berkeley, CA, USA, [3]Pacific Coastal and Marine Science Center, United States Geological Survey, Santa Cruz, CA, USA

Abstract Sea level rise (SLR) is placing both immediate and long-term pressures on coastal communities to take protective actions. Projects in the United States, and in many locations throughout the world, generally involve local jurisdictions raising the elevation of shoreline protection elements, with limited or no analysis of the feedback between shoreline management decisions and the impacts to water levels regionally. Our study examines the impact of local shoreline development on regional flood risk and considers SLR scenarios up to 1.5 m using a large-scale numerical model, as an example, for San Francisco Bay. Here we show that measures to prevent flooding along an embayment shoreline in one location or subregion may increase inundation elsewhere in the system. The network of interactions occurs not only within subbasins of the Bay but also across the greater geographic extent from one end of the Bay to the other, and local jurisdiction may have either reciprocal relationships with or asymmetric impacts on one other. Importantly, the nature of the interaction network is seen to evolve with SLR: interactions are purely subregional at current sea level but with higher sea level (e.g., 1 m of SLR), not only do the subregional interdependencies strengthen but also regional interdependences emerge.

1. Introduction

Over 600 million people currently live in the coastal zone (Neumann et al., 2015), and estimates of future flood risk due to climate change will disproportionately affect the world's major cities, many of which are situated along low-lying, estuarine shorelines (e.g., Guangzhou, Mumbai, Bangkok, and New York; Hallegatte et al., 2013). In addition, the cumulative damage of "nuisance flooding," which occurs during high tides with sea level rise, has a potential to exceed the storm floods as climate change intensifies (Moftakhari et al., 2017). Therefore, it is paramount that we better understand the influence of local estuarine shoreline infrastructure planning on regional flood risk.

Plans to mitigate or prevent flooding and inundation impacts are being developed by a wide range of actors, including private property owners, cities, counties, and regional agencies. Decision making on these projects is usually made locally. Previous studies (Bertin et al., 2014; Holleman & Stacey, 2014; Lee et al., 2017; Pelling & Green, 2014) showed that actions at particular locations can have disproportionate impacts at others. For example, Holleman and Stacey (2014) showed that shoreline protection in South San Francisco Bay could raise the maximum water level in regions to the north up to 0.2 m due to the interaction of tidal dynamics with the shorelines. However, almost no current local decision considers the impact of shoreline decisions on water levels regionally. In addition, the spatial interdependence among locations and the variation of the interaction as sea levels rise remains to be understood. To coordinate regional efforts that defend against present-day coastal flooding and the increased risk due to projected sea level rise, the impact of county or city level shoreline alternation on the regional flooding risk should be examined, and how such a local-regional coupling relationship evolves with future sea level rise scenarios must also be considered.

The scale of flooding impacts is associated with the topography of coastal areas and the water level relative to coastal protection infrastructure, with low-relief coastlines being the most vulnerable to widespread coastal flooding as infrastructure is overwhelmed. Coastal water levels are determined by a combination of factors, including mean sea level, tidal forcing, and shorter time scale events due to storms, low pressure systems, or winds (Wang et al., 2017). The mean sea level includes both long-term trends, due to sea level rise

and climate change, and natural climatic variability, with time scales ranging from months (Wolter, 1987), decades (Mantua et al., 1997) or longer. The global sea level rise has been shown to be 1.5–3.4 mm/year (Church et al., 2004; Domingues et al., 2008; Rahmstorf, 2007) and expected to accelerate in the future (Church & White, 2006). Although the rate of sea level rise varies spatially across the world due to a variety of factors in the world (Church et al., 2004; Nicholls & Cazenave, 2010), we consider here water level variability within a coastal embayment, so that we can use a specified sea level at the mouth to analyze the impacts of management actions on regional water levels. High water events at the synoptic or seasonal time scale have been examined (e.g., Lin et al., 2012; Wang et al., 2017) and found to be sufficiently independent of long-term sea level rise so that their effects can be superposed linearly. The within-bay variability of the tidal amplitude, on the other hand, is determined by the local tidal energy and its dissipation or amplification through interaction with the embayment. Our analysis focuses on the water level response to the interplay between long-term variability in sea level, estuarine shorelines and tidal dynamics, with an emphasis on the detailed spatial interactions that develop within the embayment.

In estuaries with large tidal ranges, high water events are strongly influenced by local tidal amplitude, which is shaped by the interaction of oceanic tides with the basin geometry and shorelines (Friedrichs & Aubrey, 1994; Holleman & Stacey, 2014). Tides propagate into coastal embayments as waves, which may be amplified by convergences in the basin and reflected by interactions with shorelines. Reflected waves interact with the incoming waves and, depending on the basin's depth and length, may create resonant conditions that further amplify the tides (Ippen, 1966). These two amplification mechanisms are offset by tidal dissipation by friction at the bed or along boundaries, such as beaches, wetlands, or structures. The balance of amplification and dissipation processes determine local tidal amplitudes within the Bay, which may have significant variability depending on the size, shape, spatial structure, and shoreline geomorphology of the basin. Because of the dominant role that the shape and shorelines of an embayment plays in establishing tidal conditions, the configuration of coastal protection infrastructure is a critical factor to be considered (Holleman & Stacey, 2014); in this study we examine how spatially disaggregated shoreline protection strategies interact to define regional flood conditions, with consideration of how adaptation to sea level rise interacts between jurisdictions.

Long-term changes in sea level interact with the shorelines of embayments, potentially transforming them as ocean level rise. Rising water levels would, in the absence of shoreline interventions, inundate new areas around the perimeter of the basin. This expansion of shallow water regions would feedback into the tidal dynamics through increased dissipation of energy and, potentially, decrease the likelihood of tidal amplification by the shorelines and basin geometry, which would in turn reduce local tidal amplitudes and provide regional mitigation of inundation risk or extent.

The current coastal morphology responds dynamically to shifts in sediment supply and transport and to variation in coastal forcing. As sea levels rise, the hydrodynamics will respond to the new water levels, which will lead the coastal morphology to adjust, but changes in the morphology simultaneously feedback into the hydrodynamics (Passeri, Hagen, Medeiros, Bilskie, Alizad, et al., 2015). Accurate simulation of hydrodynamics and morphological response under sea level rise, therefore, depends on the detailed resolution of both the short time scale response of the currents and waves to changes in water levels and the longer-term response of the morphology to these changes in the fluid motions. This issue is highlighted by the recent paper of Passeri, Hagen, Medeiros, and Bilskie (2015), who simulated the past hydrodynamics with historical sea levels and morphological data. Comparing the simulations between the past and present, they concluded that the coastal morphology plays an important role in predicting future sea level rises. Additionally, Bilskie et al. (2014) examined the dynamics of storm surge with the past, present, and future sea levels and morphological conditions. They discovered that storm surge is sensitive to morphological change. To address this issue, a few morphological models are incorporated into hydrodynamic models to simulate the future hydrodynamics. Passeri, Hagen, Bilskie, and Medeiros (2015) defined future shoreline conditions by extrapolating the historical records of shoreline topography. They found that the projected shoreline changes did not alter tidal ranges but influenced tidal prisms depending on the change of the bay planform. Passeri et al. (2016) used a Bayesian Network model to predict the coastal morphology and found that the coupled effects of sea level rises and morphological change can make a nonlinear impact on the projected hydrodynamics under different sea level rises.

As the geomorphology of an embayment evolves in conjunction with hydrodynamic changes, a second feedback loop emerges between the geomorphology and nearshore ecosystem development. The presence

or absence of tidal marsh habitat depends on the elevation of the estuary's bed, but the accumulation of sediment to provide bed accretion is facilitated by the presence of marsh vegetation. A major concern is the risk of loss of coastal marsh habitat due to rapid sea level rise overwhelming the ability of marshes to accumulate sediments (Craft et al., 2009; Neumann et al., 2015). Bilskie et al. (2016) extended the studies described in the previous paragraph by incorporating this feedback in a hydrodynamic-ecological model to predict the future marsh distribution. Introducing representative historical hurricanes, they found significant increase of inundation areas with the projected coastal morphological condition and future sea levels, even when accounting for the development of tidal marshes. Alizad et al. (2016) performed a detailed study on the marsh response to the sea level rise using a marsh productivity model. They found that the biomass density in the low sea level rise scenario was relatively uniform with modest variation but suffered a heavy loss with higher sea levels.

In the face of all of these complex feedbacks, we now wish to introduce an additional one that influences the regional management of the shorelines of tidal embayments. That is, management decisions about where, and to what extent, to accommodate inundation under future sea level scenarios will influence the tidal dynamics of embayments and lead to regional responses in water levels and inundation. These changes in the water level, and the extent of new inundation, will feedback into the hydrodynamics and influence the tidal currents, residual flows, and wave motions, which will lead to longer-term adjustment of the geomorphology and perimeter ecosystems through the feedbacks described above. The present study, however, focuses on the geographic feedback that emerges through the water levels themselves due to shoreline management decisions about how, and to what extent, to accommodate rising sea levels. The goal of this work is not to comprehensively resolve the evolution of a tidal embayment, its morphology, and its ecosystem conditions in response to rising sea levels but rather to evaluate the change of regional flooding risk for various shoreline alternatives based on real political jurisdictions. We emphasize that the present study, which uses San Francisco Bay as a case study, is not intended to simulate and predict the details of the hydrodynamics with the future sea level scenarios and a fully coupled morphologic-hydrodynamic-ecosystem model is beyond our scope. Instead, we simplify our analysis to make use of current coastal topography and tidal forcing, but with higher mean sea levels, in order to focus our attention on the interaction of shoreline actions and inundation responses around the Bay. This research has implications for the societal response to sea level rise globally, especially for the tens of millions of people who currently live in the coastal floodplain of the heavily urbanized embayments across the world. Given projections of sea level rise and population growth, the population at risk of coastal flooding could more than double by the middle of the 21st century (Neumann et al., 2015), further stressing the importance of identifying region solutions to mitigate the impacts of sea level rise.

2. Simulation of Coastal Flooding

San Francisco Bay is surrounded by nine counties, that is, San Francisco (SF), Sonoma (SN), Alameda (AL), Santa Clara (SC), Solano (SL), Contra Costa (CC), Marin (MR), San Mateo (SM), and Napa (NP). Each county has an area of jurisdiction as shown in Figure 1, which covers both lands and waters. Alameda, Santa Clara, and San Mateo counties form what is frequently referred to as South San Francisco Bay, which features a highly urbanized shoreline including residential and commercial districts, including technology giants such as Google, Facebook, and Apple, as well as critical transportation and other supporting infrastructure. The northern portion of San Francisco Bay consists mainly of two tidal basins: San Pablo Bay on the west and Suisun Bay on the east. The latter connects to the Sacramento-San Joaquin Delta area. The relative position and topography of the counties lead to complicated reciprocal relationships in the tidal hydrodynamics, which requires a large-scale numerical model to fully investigate.

Modeling the interaction between tidal dynamics and coastal protection infrastructure under various sea level rise scenarios requires a flexible numerical scheme that is able to incorporate the irregular, fine-scale details of the shorelines, including both managed levees or seawalls and natural marshes, beaches or other habitats. To ensure effective resolution of these complex shorelines, this study employs the Deltares D-Flow Flexible Mesh software, which numerically solves the 2-D shallow water equations and parameterizes seawalls and levees using empirical weir models (Deltares, 2015). Because the mesh is unstructured, the grid orientation can be can be made to efficiently incorporate coastal protection infrastructure. A drying and wetting algorithm is employed to incorporate the coastal dissipation and tidal flooding. The validation results are summarized in Appendix A. A detailed validation of the numerical scheme can be found in Wang et al. (2017)
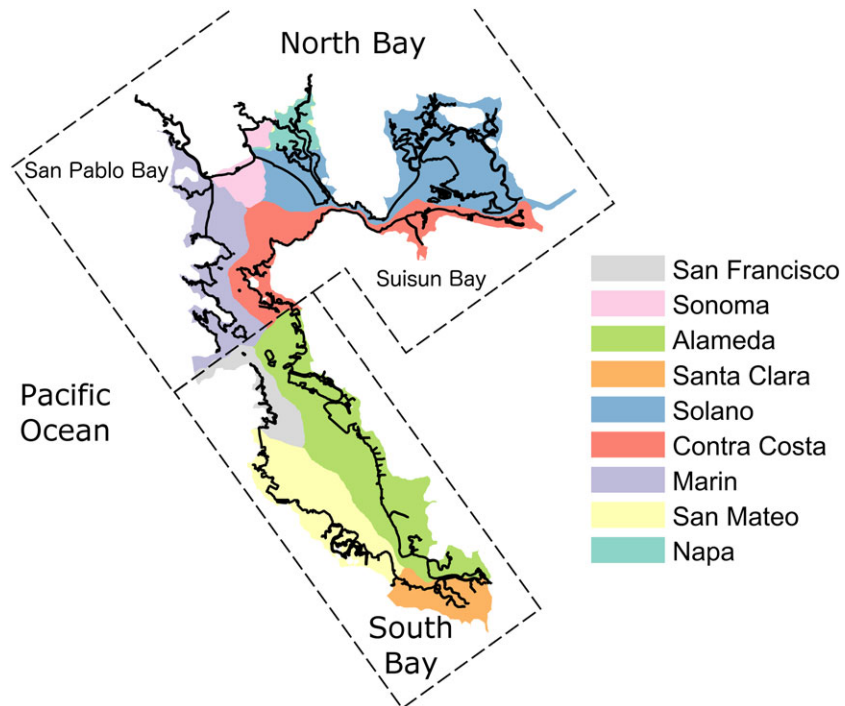
Figure 1. Jurisdiction areas of the nine counties of San Francisco Bay. Each county includes a jurisdiction area covering lands and waters. The solid line shows the existing land boundary.

and the construction and validation of the Coastal Storm Modeling System across the region (Barnard et al., 2014; Elias & Hansen, 2013; Erikson et al., 2013; Martyr-Koller et al., 2017). About 250 levees and seawalls (Doehring et al., 2016) are incorporated in the simulation to reproduce the existing shoreline configuration and 11 river discharges (McKee et al., 2013) are introduced to simulate the major freshwater sources in the area. The different sea level rise scenarios are implemented by adjusting the mean water level at the open ocean boundary.

Future shoreline protection strategies can be broadly categorized into two types: accommodation and containment. "Accommodation refers to a shoreline strategy that allows rising coastal waters to inundate new areas, which in many cases will create broad shallow regions along the estuarine perimeter. Containment refers to strategies that maintain existing shorelines through the construction of barriers to contain the estuarine waters based on the current configuration of the shoreline. We refrain here from referring to these two approaches using the commonly used terms "softening" and "hardening" due to the fact that accommodation strategies may involve hardscape (urban development that is allowed to intermittently flood) and containment strategies may involve natural landscapes (levee and marsh complexes). The key distinction for the analysis we present here is *where* the shorelines are prescribed, not the details of how the shoreline is constructed. The distinction between accommodation and containment becomes particularly pronounced under scenarios of future sea levels, where increases in water levels would lead the estuarine waters, if not contained, to inundate new regions. In the coming century, coastal communities around the world will be facing the fundamental decision as to whether to maintain existing shorelines through a containment strategy or to accommodate expanded inundation through adaptation of existing infrastructure systems. In our analysis, we use the San Francisco Bay Area as a case study to illustrate the dynamics and tradeoffs that are created by this decision.

This study considers the spatial interaction of local and independent coastal protection decisions. Specifically, we use the construct of the nine counties with San Francisco Bay shoreline to define the scale of decision making. We assume that a county has autonomous authority to create new or elevate existing seawalls to protect its current land area. Our scenarios then involve individual actors (counties) choosing to construct a shoreline containment structure (sea wall or levee) along its entire shoreline in order to assess the relationship with regional water levels. In the numerical model, these containment structures are assumed to be robust to any
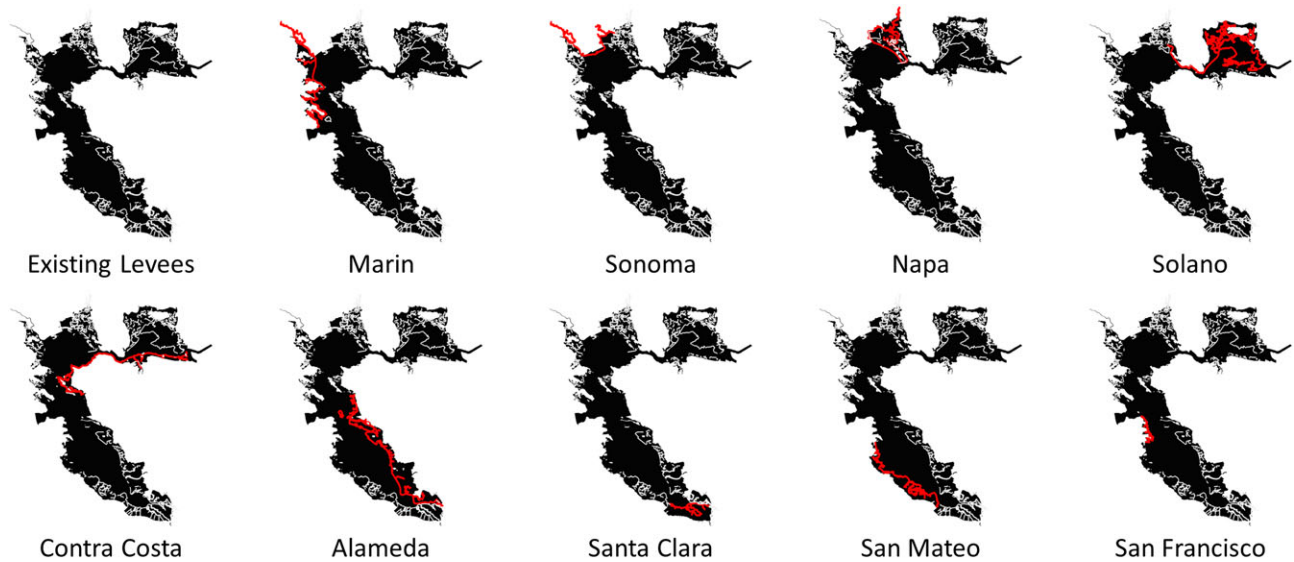
Figure 2. Hypothetic shoreline protection scenarios. Contiguous seawalls are assumed to be built along the land boundaries of each county (red lines). Existing shoreline structures are represented by a gray line. Including the existing shoreline configuration, 10 protection scenarios are developed.

future condition and are imposed as absolute flow barriers. The shoreline protection scenarios for the different counties of San Francisco Bay are shown in Figure 2. This study examines the impact of the hypothetical county-scale seawall on the subregional and regional hydrodynamics.

3. Methods

High-resolution numerical simulations of tidal hydrodynamics within San Francisco Bay were done using the Deltares D-Flow Flexible Mesh (DFM) hydrodynamics model. This numerical model implements an unstructured mesh with resolution as fine as 50 m, which allows incorporation of major levees and seawalls (Figure 3). The governing equations of the model are the 2-D shallow water equations,

$$\frac{\partial h}{\partial x} + \frac{\partial Uh}{\partial x} + \frac{\partial Vh}{\partial x} = hQ, \tag{1}$$

$$\frac{\partial U}{\partial t} + U\frac{\partial U}{\partial x} + V\frac{\partial U}{\partial x} = -g\frac{\partial \zeta}{\partial x} + \nu\left(\frac{\partial^2 U}{\partial x^2} + \frac{\partial^2 U}{\partial y^2}\right) - \frac{1}{C^2}\frac{g}{h}U\left|U\right|, \tag{2}$$

$$\frac{\partial V}{\partial t} + U\frac{\partial V}{\partial x} + V\frac{\partial V}{\partial x} = -g\frac{\partial \zeta}{\partial y} + \nu\left(\frac{\partial^2 V}{\partial x^2} + \frac{\partial^2 V}{\partial y^2}\right) - \frac{1}{C^2}\frac{g}{h}V\left|V\right|, \tag{3}$$

where U and V are the depth averaged velocities, h is the water depth, t, x, and y are the time and spatial coordinates, Q is the contributing discharge per unit area, g is the gravitational acceleration, ζ is the water level, ν is the eddy viscosity, and C is the drag coefficient.

The containment strategy, which consists of maintaining existing shorelines in perpetuity, is imposed using a completely contiguous infinitely high seawall. More details can be found in the Deltares Flexible Mesh Technical Reference Manual (Deltares, 2015).

To create the shoreline scenarios, we assume a series of jurisdiction rules to break down the coastline into nine counties. First, the land boundary of the continent is divided into different counties according to the land area division. Second, the shoreline of an island is always kept complete and assigned into the same county. If the shoreline of an island crosses the boundaries of more than one county, the county that has the longest shoreline is assumed to govern the whole island's coastline. These rules are set to ensure the coherence of land protection and avoid unnecessary floods due to break points of a continuous protection. Note that these rules are for computing convenience and do not reflect the practical management rights of the counties.
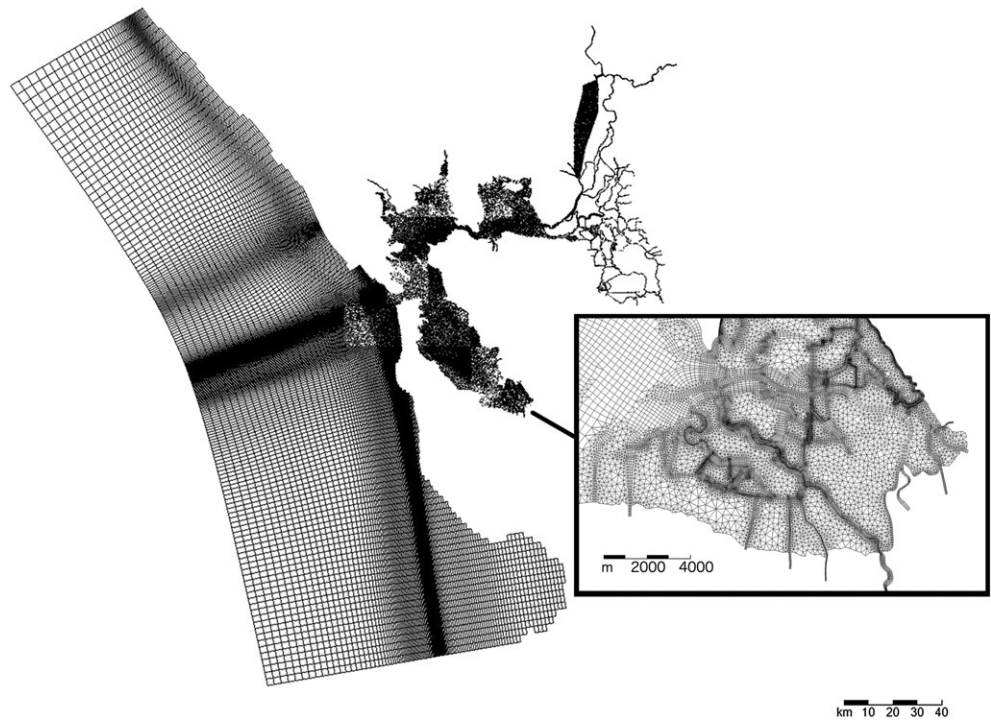
Figure 3. Grid of the computational domain. The insert is a zoom-in of the south end of the bay.

To estimate the spatial interdependence (as summarized in the matrix and network figures), the total flood volume is calculated using the integral,

$$V = \int_{S_{in}} \Delta\zeta \, dS, \tag{4}$$

where V is the total volume of flood water change, S_{in} is the inland area of a county, and $\Delta\zeta$ is the depth of the inundated region. A matrix representation of the spatial interdependence of total flooding volume is shown in Figure 4. The values represent the volume of new inundation waters accumulated at one county due to a shoreline protection action by another; as a result, higher values represent stronger spatial interactions. The results in Figure 4 represent the raw inundation data and are not normalized to account for the size of various counties (see Figure 6 and associated discussion below for the normalized results).

The equivalent flooding penetration distance is calculated using equation

$$\frac{1}{2}LD^2S = V, \tag{5}$$
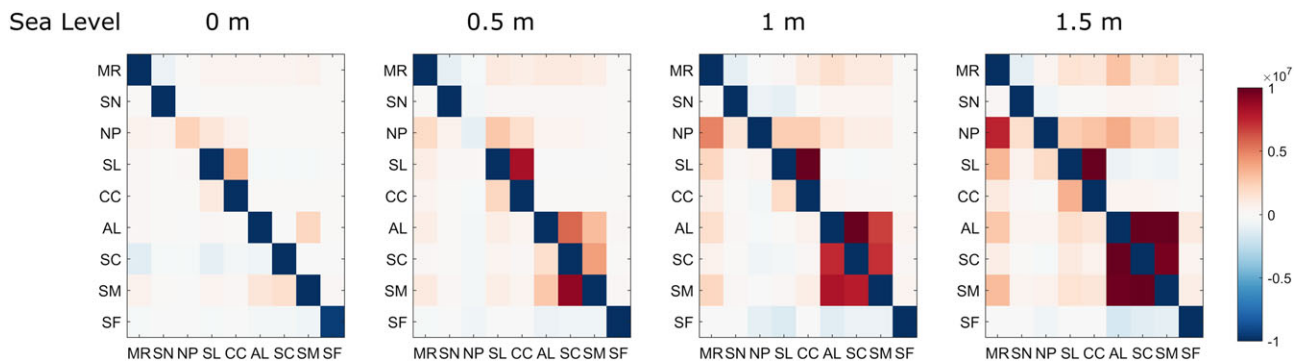

Figure 4. Matrix of spatial interdependence. The color of the block shows the volume of new inundation waters in one county due to the pursuit of a containment strategy by another county. The vertical axis represents the county that takes action, and the horizontal axis represents the county that is impacted by the protection action. The color bar is in units of cubic meters.

Table 1
Shoreline Length and Average Coastal Slope of Each County

County	Shoreline length (km)	Average slope ($\times 10^{-3}$)
Alameda	268	7.2
Contra Costa	200	17.2
Marin	251	15.3
Napa	138	5.2
Santa Clara	100	8.1
San Francisco	56	16.4
Solano	505	8.7
San Mateo	176	5.1
Sonoma	121	5.6

where L is the length of the shoreline (see Table 1), D is the average increased penetration distance, S is the average slope of the coastal area, and V is the total volume of increased flooding water in the land of a county. We drew 2×10^9 transects normal to the shoreline with equal distance to each other and 100 m into the sea and the land. The elevation of 201 points along each transect was collected, and the average slope of a county is derived by the linear regression of these points. We checked the convergence of this method by observing the change of the slope when increasing the number of transects. The obtained slope of each county is listed in Table 1.

4. Quantifying Impacts of Shoreline Scenarios on Inundation

Numerical simulations are carried out for all coastal protection scenarios with sea level rise heights of 0, 0.5, 1, and 1.5 m above present day. This range of sea level rise covers the main trend of sea level rise projections in 2100 (Stocker, 2014). In each sea level rise scenario, a control case is prepared by simulating the tidal dynamics with the existing shoreline configuration. The water level of the control is then subtracted from the other simulation cases that share the same sea level rise scenario to show the change of the maximum water level throughout the Bay as shown in Figure 5. In this way, we are quantitatively defining the spatial impacts of a county's individual action for a particular future sea level scenario.

In spite of the fact that the containment strategy for a county is intended to simply preserve current shorelines, the definition of existing shorelines is not always clear due to tidal variability and fringing intertidal regions. At the same time, we wanted to be certain that future conditions under the containment strategy did not involve any new inundation. As a result, when this boundary was unclear, the barriers shown in Figure 2 were chosen to be further into the Bay to ensure future conditions truly represented containment. The result of this decision is that even under current sea levels there is a hydrodynamic effect of a county's containment action (see row 1 of Figure 5). The fact that certain counties (most notably San Mateo, Santa Clara, Marin, and Alameda) have a clear impact on estuarine water levels is due to their position in the estuary and the specification of a hard boundary that intrudes into the intertidal perimeter of the estuary. These results for current sea level will be used as a baseline for discussion of the impacts of future sea level interactions with shoreline scenarios (the other row two through four in Figure 5).
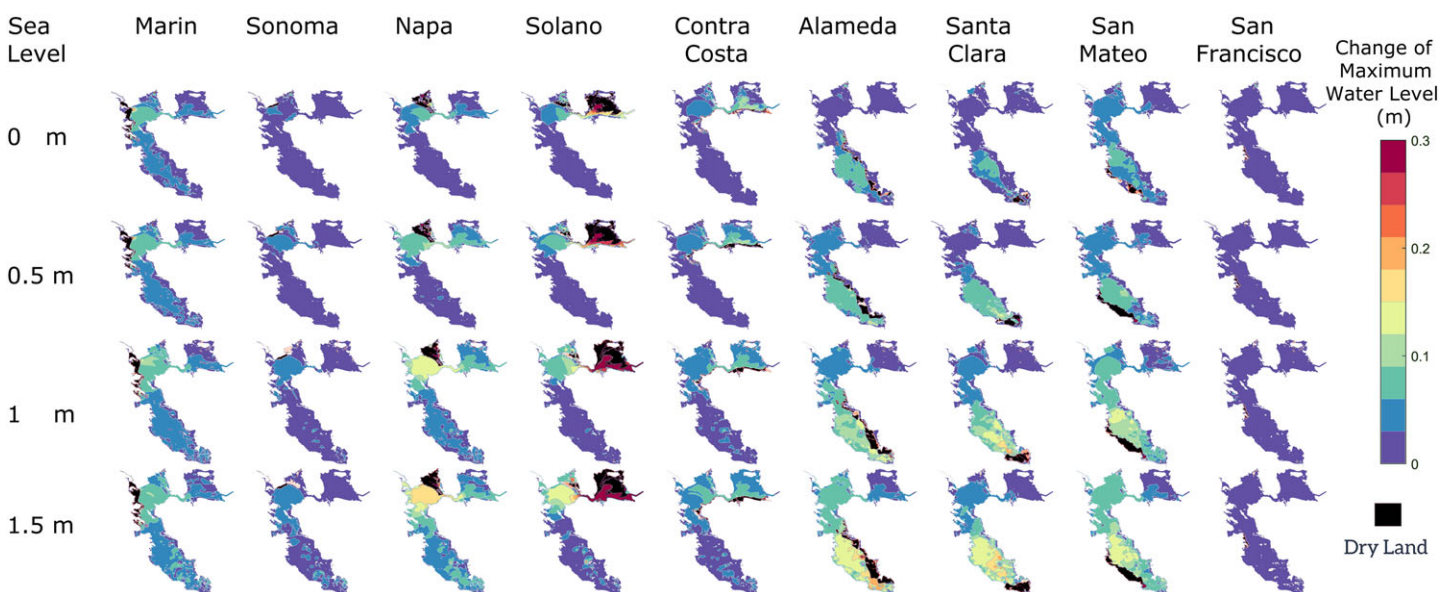
Figure 5. Spatial distribution of the change in maximum water level when each shoreline scenario is imposed. Each case is derived by subtracting the maximum water level of the case that simulates the existing shorelines from the maximum water level for a case where a shoreline protection scenario was applied. The darker blue represents greater maximum water level rise. The black area is the emerged dry region that is protected by the shoreline scenario.
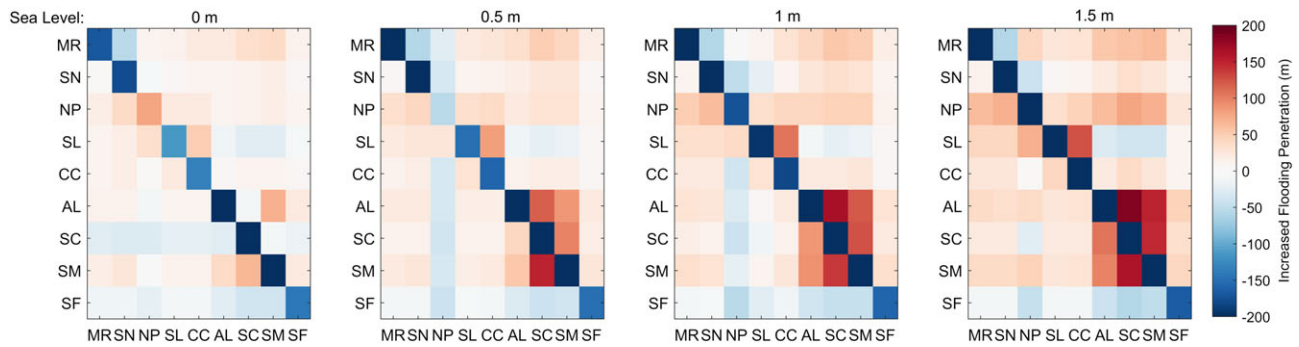
Figure 6. Matrix of spatial interdependence. The color of the block shows the equivalent penetration distance of new inundation waters in one county due to the pursuit of a containment strategy by another county. The vertical axis represents the county that takes action, and the horizontal axis represents the county that is impacted by the protection action. The color bar is in units of meters.

To understand the impact of a county's action on other counties in the region, for each shoreline scenario, we integrate the volume of water that enters the inland area for each county in the region. This volume represents the new inundation of each county due to the action of each of the other counties to maintain existing shorelines. An equivalent average flooding penetration distance was calculated using the average slope at each county's shoreline and the total increased flood volume (more details about the equivalent penetration distance can be found in section 3). The county-by-county, action-to-response results can be presented in matrix form (Figure 6) in which the vertical axis represents the county that is taking action to maintain its shoreline, and the horizontal axis is the county in which the impact is being quantified. The diagonal cells therefore represent the protection of a county's land area by its own action and is therefore negative (a reduction in inundation) in all cases except for Napa under current sea level conditions. This anomalous result is due to cross-jurisdictional rivers that provide an alternative path for inundation, but the result does not persist under future scenarios (our focus in this study) nor does it affect other counties in the region. The off-diagonal cells show the impact of coastal protection actions on other counties and therefore represent the spatial interactions between management actions and flood impacts. In general, impacts are greatest in nearby counties, which appear near the diagonal in Figure 6; these results will be discussed in more detail in the next section. Note that the equivalent flooding penetration distance is a parameter that is averaged over the whole shoreline of a county. The penetration distance of flooding event at a particular location could be extraordinarily severe than the average.

As an alternative to the matrix structure, the spatial interactions in the region may be more intuitively presented as a geographic network, where directional links are defined when the new inundation volume

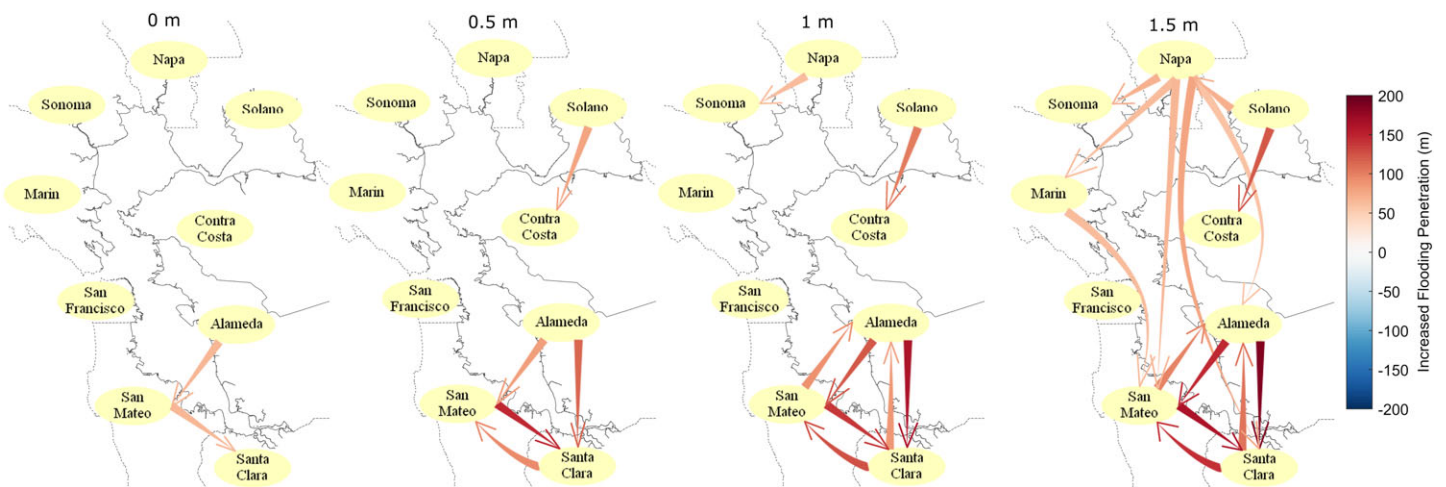**Figure 7.** Network of the strong spatial interdependence. Links are shown when the equivalent penetration distance of new inundation is greater than 60 m. The thin head of the edge points to the county that is impacted and the thick head is placed at the county that takes an action. The color of the edge shows the average penetration distance of the total flood water change, and the scale is shown using the color bar on the right.

in a county exceeds a threshold (Figure 7). The colors of the links in the network show the total flood water volume change induced by the action of one county, with the thick end of the link placed at the county taking action and the thin end at the county experiencing the impact (i.e., the links "point" from action to response).

5. Descriptions of Sea Level Rise and Shoreline Infrastructure Decisions

Within each column of Figure 5 the effects of interaction of sea level rise with shoreline infrastructure is illustrated through the spatial distribution of maximum water levels. In general, as sea levels rise, the effects of shoreline interventions become larger and more geographically distributed. Alameda county perhaps provides the most glaring example of this dynamic, as the impacts on water level are highly localized under current sea levels, but the influence of the county maintaining its shoreline begins to extend throughout the Bay and becomes increasingly intense in the southern part of the Bay, as sea level is increased by 1 or 1.5 m over the present day. The interjuridicational interactions are qualitatively similar for all counties: under current conditions, the effects of shoreline actions are highly localized, but as sea levels rise, the interactions become stronger and increasingly subregional (within a subembayment) or regional.

There are several specific responses that can be considered through comparison of the various shoreline scenarios. Solano and Contra Costa counties, for example, appear to have only local or subregional (i.e., limited to the northern part of the Bay) effects on water level even for the most extreme sea level scenarios. Conversely, other counties have a regional influence even under modest sea level scenarios while others have strongly increasing influence as sea levels rise. Specifically, Marin and San Mateo counties have a subregional and regional influence under the modest sea level rise scenario. In contrast, Napa county (in North Bay) and Alameda and Santa Clara counties (in South Bay) have weak subregional influences for modest sea level rise but actually exceed the influence of Marin or San Mateo county for 1 and 1.5 m of sea level rise.

To focus specifically on the geographic interaction between decision makers (i.e., counties), we turn to the matrices of Figure 6. In general terms, as sea levels rise, more off-diagonal cells become positive, which quantifies the increasing interdependence of counties as they adapt to higher sea levels. Subregionally (i.e., within North Bay or within South Bay), intense bidirectional interactions emerge as seas rise, which can be seen by the positive three-by-three submatrix describing the interdependence of Alameda, Santa Clara, and San Mateo counties. A similar interdependence is evident between Solano and Contra Costa counties and, to a lesser extent, Marin and Napa counties. These interactions reflect the basin-scale dynamics that govern the tides. In South Bay, when containment strategies are pursued, the tides are amplified (relative to accommodation strategies) by the two physical processes outlined: a focusing of tidal energy into smaller cross-sectional area and resonance between the basin and the tidal forcing. Similarly, in North Bay, Marin, and Napa counties are linked to one another dynamically, as are Solano and Contra Costa counties. These subregional interactions intensify with increasing sea level rise.

In the case of the extreme sea levels, we note the appearance of significant regional interactions that connect North Bay and South Bay. Specifically, actions by Marin and Napa counties to maintain current shorelines influence a number of South Bay counties in the case of 1.5 m of sea level rise (the top row and the third row in the right-hand panel of Figure 6). Similarly, containment strategies by San Mateo and Alameda (second and fourth rows from the bottom of the right panel in Figure 6) influence Napa county and, to a lesser extent, Marin, Sonoma, Solano, San Francisco, and Contra Costa counties. These regional interdependencies are created by the subregional tidal dynamics feeding into the boundary condition for the other subregion. In other words, under the extreme scenario, the shoreline containment strategies in the South Bay have a strong enough dynamical effect to alter water level conditions in the Central Bay, which defines the boundary condition for the North Bay, an ultimately amplifies water levels as well. The reverse also appears in the matrix description of interdependence.

These subregional and regional interactions are evident in the geographic network, Figure 7. At modest sea levels (0–1 m), interdependence links are limited to weak subregional interactions. As sea levels rise by 1.5 m; however, the subregional interdependencies become more intense (the clusters of red arrows in the southern and northern portions of the Bay in the right two panels of Figure 7) and regional interdependencies appear (links between Marin and Napa counties in the north with Santa Clara and San Mateo counties in the south).
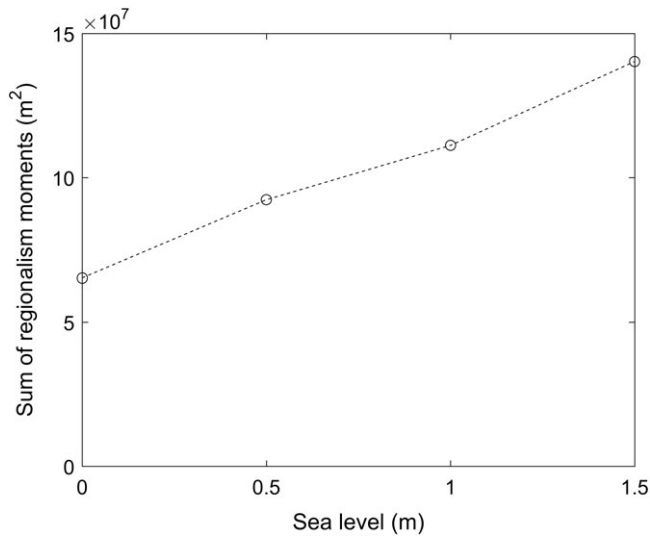
Figure 8. Increasing trend of the regionalism moments at different sea levels.

6. Interpretation of Regional Interactions

Using the county-by-county results from the previous section (Figures 6 and 7), there are some important differences that can be emphasized. First of all, in the South Bay, where tidal amplification and shoreline interactions are strongest (Holleman and Stacey), subregional interactions are most pronounced, even at moderate sea level scenarios. In the North Bay, subregional interactions are present in San Pablo Bay, but counties to the east (Solano and Contra Costa Counties) have only local, or very weak subregional, interactions with their neighbors. These differences can be understood through the tidal dynamics of the embayments: South Bay and San Pablo Bay are both characterized by tidal amplification and positive feedback between tidal amplitudes and their shorelines; Suisun Bay, on the other hand, is highly dissipative of the tides due to its braided channel structure. As a result, shoreline alteration by communities in Suisun Bay is less likely to have regional impacts than would similar actions on the other subembayments.

We are interested now in understanding how the Bay Area transitions from local to subregional to regional interactions. While the matrix and network results illustrate this evolution of the system, we now consider the definition of an aggregated measure of the strength of regional interactions, which we refer to as the Regionalism Moment (R_m). Regionalism moment is defined as a product of the penetration distance from above and the distance between the action and the receiving counties, that is,

$$R_m = \Sigma |L_p| \times L_c, \tag{6}$$

where L_p is the average penetration distance for a county, L_c is the distance between counties, and the summation is over all action-response pairs (Figure 6). The result of these calculations is shown for our four sea level scenarios in Figure 8. While four scenarios are insufficient to accurately capture the transitions that occur in the system, combining this result with the matrix and network illustrations allows us to interpret the system as transitioning from local interactions (current sea level) to subregional interactions (0.5 and 1.0 m) to regional interactions (1.5 m). In R_m, these transitions are evident in the more rapid increases between 0 and 0.5 m and between 1.0 and 1.5 m; if the geographic interactions were not growing, the methods used to calculate penetration length would result in a constant increase between these four sea level scenarios.

7. Conclusions

The geographic network of actions and response in San Francisco Bay provides a quantitative illustration of the interdependence of sea level rise adaptation in coastal embayments worldwide. The nature of tidal hydrodynamics creates a feedback between basin shorelines and geometry and tidal inundation which is influenced by the long-term evolution of sea level. As sea levels rise, geographic interdependence becomes more intense and widespread so that counties (or other distributed decision makers) must have knowledge of, or make assumptions about, the actions others will take while making their own adaptation plans. This bidirectional interdependence is not necessarily symmetric, however, and some locations or shorelines have disproportionate regional influence.

In the shoreline scenarios analyzed here, it is important to note that only one county takes action at one time. In any coastal region, it is expected that shoreline interventions will be pursued simultaneously, whether coordinated or not. The current study explores the individual influence of a county on the region, and the coordinated or simultaneous action of multiple counties would not necessarily be linearly additive. Additional simulations are required to evaluate the regional impact of multiple, variable protection strategies, which may include consideration of the "optimal" strategy that would be pursued by an omniscient regional decision maker.

It is also important to note that this analysis is only the first step to understanding the complex feedbacks that exist and shape coastal tidal embayments as they evolve in response to rising sea levels. The water levels described here would shape changes in local tidal flows and wave dynamics, possibly with implications

Table A1
Comparisons of Water Levels for Validation

Station name	r	Lag (s)	RMS ratio
Point Arena	0.9996	−122	1.001
Monterey	0.9993	−120	0.986
San Francisco	0.9952	98	1.033
Alameda	0.9970	193	1.027
Richmond	0.9971	−433	1.017
Redwood City	0.9960	202	1.002
Coyote Creek	0.9923	−259	0.973
Port Chicago	0.9885	−530	1.052
Martinez	0.9862	−420	0.969

for the residual circulation in the basin. These hydrodynamic changes would interact with geomorphological and ecological processes to define the more complete evolution of the embayment (Bilskie et al., 2016; Passeri et al., 2016). From the perspective of managed shorelines, these processes and feedbacks would define the sustainability of coastal interventions, with implications for maintenance costs and effectiveness.

The regional interactions identified in this paper due to local and regional shoreline infrastructure decisions would be expected to develop in other tidal embayments, although the quantitative details will certainly be different. Tidal physics in estuaries are strongly influenced by the basin geometry (shorelines and depth variability), which determines the amplification and dissipation of tidal energy. In smaller (shorter) estuaries, the feedback between shorelines and tidal dynamics will be more limited. In large systems, however, the potential for feedback is pronounced and spatial interactions between adaptation measures should be evaluated. Many of the largest cities across the world are situated along these types of large-scale estuarine shorelines, and therefore, the dynamic interaction of coastal flood protection actions with tidal hydrodynamics must be carefully evaluated in order to accurately assess and reduce future flood risk.

Appendix A

The present numerical model is validated against the water level at nine stations recorded by NOAA in San Francisco Bay. The validation results are quantified in Table A1. All of the comparisons are satisfactory. The r denotes the Pearson correlation coefficient. Lags are computed as the time offset that maximizes the correlation coefficient. The RMS ratio is the ratio of model RMS amplitude to observed RMS amplitude. More validation details can be found in Wang et al. (2017).

References

Alizad, K., Hagen, S. C., Morris, J. T., Medeiros, S. C., Bilskie, M. V., & Weishampel, J. F. (2016). Coastal wetland response to sea-level rise in a fluvial estuarine system. *Earth's Future*, *4*, 483–497. https://doi.org/10.1002/2016EF000385

Barnard, P. L., van Ormondt, M., Erikson, L. H., Eshleman, J., Hapke, C., Ruggiero, P., et al. (2014). Development of the coastal storm modeling system (CoSMoS) for predicting the impact of storms on high-energy, active-margin coasts. *Natural Hazards*, *74*, 1095–1125.

Bertin, X., Li, K., Roland, A., Zhang, Y. J., Breilh, J. F., & Chaumillon, E. (2014). A modeling-based analysis of the flooding associated with Xynthia, central Bay of Biscay. *Coastal Engineering*, *94*, 80–89.

Bilskie, M. V., Hagen, S. C., Alizad, K., Medeiros, S. C., Passeri, D. L., Needham, H. F., & Cox, A. (2016). Dynamic simulation and numerical analysis of hurricane storm surge under sea level rise with geomorphologic changes along the northern Gulf of Mexico. *Earth's Future*, *4*, 177–193. https://doi.org/10.1002/2015EF000347

Bilskie, M. V., Hagen, S. C., Medeiros, S. C., & Passeri, D. L. (2014). Dynamics of sea level rise and coastal flooding on a changing landscape. *Geophysical Research Letters*, *41*, 927–934. https://doi.org/10.1002/2013GL058759

Church, J. A., & White, N. J. (2006). A 20th century acceleration in global sea-level rise. *Geophysical Research Letters*, *33*, L01602. https://doi.org/10.1029/2005GL024826

Church, J. A., White, N. J., Coleman, R., Lambeck, K., & Mitrovica, J. X. (2004). Estimates of the regional distribution of sea level rise over the 1950–2000 period. *Journal of Climate*, *17*(13), 2609–2625.

Craft, C., Clough, J., Ehman, J., Joye, S., Park, R., Pennings, S., et al. (2009). Forecasting the effects of accelerated sea-level rise on tidal marsh ecosystem services. *Frontiers in Ecology and the Environment*, *7*(2), 73–78.

Deltares (2015). *Delft3D flexible mesh suite. D-flow flexible mesh. Technical reference manual*. Netherlands: WL Delft Hydraulics.

Doehring, C., Beagle, J., Lowe, J., Grossinger, R., Salomon, M., Kauhanen, P., et al. (2016). *San Francisco Bay shore inventory: Mapping for sea level rise planning*. Richmond, CA: San Francisco Estuary Institute.

Domingues, C. M., Church, J. A., White, N. J., Gleckler, P. J., Wijffels, S. E., Barker, P. M., & Dunn, J. R. (2008). Improved estimates of upper-ocean warming and multi-decadal sea-level rise. *Nature*, *453*(7198), 1090–1093.

Elias, E. P., & Hansen, J. E. (2013). Understanding processes controlling sediment transports at the mouth of a highly energetic inlet system (San Francisco Bay, CA). *Marine Geology*, *345*, 207–220.

Erikson, L. H., Wright, S. A., Elias, E., Hanes, D. M., Schoellhamer, D. H., & Largier, J. (2013). The use of modeling and suspended sediment concentration measurements for quantifying net suspended sediment transport through a large tidally dominated inlet. *Marine Geology*, *345*, 96–112.

Friedrichs, C. T., & Aubrey, D. G. (1994). Tidal propagation in strongly convergent channels. *Journal of Geophysical Research*, *99*, 3321–3321.

Hallegatte, S., Green, C., Nicholls, R. J., & Corfee-Morlot, J. (2013). Future flood losses in major coastal cities. *Nature Climate Change*, *3*(9), 802–806.

Holleman, R. C., & Stacey, M. T. (2014). Coupling of sea level rise, tidal amplification, and inundation. *Journal of Physical Oceanography*, *44*(5), 1439–1455.

Ippen, A. T. (1966). *Estuary and coastline hydrodynamics*. New York: McGraw-Hill Book Co.

Lee, S. B., Li, M., & Zhang, F. (2017). Impact of sea level rise on tidal range in Chesapeake and Delaware Bays. *Journal of Geophysical Research: Oceans*, *122*, 3917–3938. https://doi.org/10.1002/2016JC012597

Lin, N., Emanuel, K., Oppenheimer, M., & Vanmarcke, E. (2012). Physically based assessment of hurricane surge threat under climate change. *Nature Climate Change*, *2*(6), 462–467.

Mantua, N. J., Hare, S. R., Zhang, Y., Wallace, J. M., & Francis, R. C. (1997). A Pacific interdecadal climate oscillation with impacts on salmon production. *Bulletin of the American Meteorological Society*, *78*(6), 1069–1079.

Martyr-Koller, R., Kernkamp, H., van Dam, A., van der Wegen, M., Lucas, L., Knowles, N., et al. (2017). Application of an unstructured 3D finite volume numerical model to flows and salinity dynamics in the San Francisco Bay-Delta. *Estuarine, Coastal and Shelf Science*, *192*, 86–107.

McKee, L., Lewicki, M., Schoellhamer, D., & Ganju, N. (2013). Comparison of sediment supply to San Francisco Bay from watersheds draining the Bay Area and the Central Valley of California. *Marine Geology*, *345*, 47–62.

Moftakhari, H. R., AghaKouchak, A., Sanders, B. F., & Matthew, R. A. (2017). Cumulative hazard: The case of nuisance flooding. *Earth's Future*, *5*, 214–223. https://doi.org/10.1002/2016EF000494

Neumann, B., Vafeidis, A. T., Zimmermann, J., & Nicholls, R. J. (2015). Future coastal population growth and exposure to sea-level rise and coastal flooding—A global assessment. *PloS One*, *10*(3), e0118571.

Nicholls, R. J., & Cazenave, A. (2010). Sea-level rise and its impact on coastal zones. *Science*, *328*(5985), 1517–1520.

Passeri, D. L., Hagen, S. C., Bilskie, M. V., & Medeiros, S. C. (2015). On the significance of incorporating shoreline changes for evaluating coastal hydrodynamics under sea level rise scenarios. *Natural Hazards*, *75*(2), 1599–1617.

Passeri, D. L., Hagen, S. C., Medeiros, S. C., & Bilskie, M. V. (2015). Impacts of historic morphology and sea level rise on tidal hydrodynamics in a microtidal estuary (Grand Bay, Mississippi). *Continental Shelf Research*, *111*(Part B), 150–158.

Passeri, D. L., Hagen, S. C., Medeiros, S. C., Bilskie, M. V., Alizad, K., & Wang, D. (2015). The dynamic effects of sea level rise on low-gradient coastal landscapes: A review. *Earth's Future*, *3*, 159–181. https://doi.org/10.1002/2015EF000298

Passeri, D. L., Hagen, S. C., Plant, N. G., Bilskie, M. V., Medeiros, S. C., & Alizad, K. (2016). Tidal hydrodynamics under future sea level rise and coastal morphology in the Northern Gulf of Mexico. *Earth's Future*, *4*, 159–176. https://doi.org/10.1002/2015EF000332

Pelling, H. E., & Green, J. M. (2014). Impact of flood defences and sea-level rise on the European Shelf tidal regime. *Continental Shelf Research*, *85*, 96–105.

Rahmstorf, S. (2007). A semi-empirical approach to projecting future sea-level rise. *Science*, *315*(5810), 368–370.

Stocker, T. (2014). *Climate change 2013: The physical science basis: Working Group I Contribution to the Fifth Assessment Report of the Intergovernmental Panel on Climate Change*. Cambridge, UK: Cambridge University Press.

Neumann, B., Vafeidis, A. T., Zimmermann, J., & Nicholls, R. J. (2015). Future coastal population growth and exposure to sea-level rise and coastal flooding—A global assessment. *PloS One*, *10*(3), e0118571.

Wang, R.-Q., Herdman, L. M., Erikson, L., Barnard, P., Hummel, M., & Stacey, M. T. (2017). Interactions of estuarine shoreline infrastructure with multiscale sea level variability. *Journal of Geophysical Research: Oceans*, *122*, 9962–9979. https://doi.org/10.1002/2017JC012730

Wolter, K. (1987). The southern oscillation in surface circulation and climate over the Tropical Atlantic, Eastern Pacific, and Indian Oceans as captured by cluster analysis. *Journal of Climate and Applied Meteorology*, *26*(4), 540–558.